Application of Electrochemical Impedance Spectroscopy (EIS) on Module Level Li-ion Batteries for Echelon Utilization

Alexandru Savca
Supervised by: Reza Azizighalehsari, Prasanth Venugopal
Faculty of Electrical Engineering, Mathematics and Computer Science(EEMCS), University of Twente
Enschede, The Netherlands

***Abstract*—The rising demand for lithium-ion batteries in the EV sector brings up ecological issues and the need for reusing the second-life lithium-ion batteries for other purposes. Thus, the battery modules have to be tested and sorted according to their state of health before being assembled in battery packs and used in their second-life application. Electrochemical impedance spectroscopy is a powerful and effective tool for characterization of batteries state of health. Due to the need of fast testing and the tendency to perform the EIS measurements on module level, it is meaningful to assess the validity of EIS on module level and if the SOH can be retrieved in the same way as for individual cells. In this paper, EIS is performed on a lithium-ion battery module with an unknown history and state of health. Curve fitting technique was used to fit the measured EIS spectra to an equivalent circuit model (ECM) to extract the circuit elements. The contribution of individual cell elements to the whole module elements was investigated and the elements sensitive to SOH were determined. The charge transfer resistance, double layer capacitance and the ohmic resistance of the individual cells were accurately reflected on the module's ECM elements. The ohmic resistance and the charge transfer resistance showed correlation to the SOH of the cells and the module.**

***Index Terms*—Lithium-ion battery(LIB), electrochemical impedance spectroscopy(EIS), equivalent circuit model(ECM), electrical vehicle(EV), state of health(SOH), galvanostatic EIS(GEIS), potentiostatic EIS(PEIS), solid electrolyte interface(SEI), frequency response analyzer(FRA)**

I. Introduction

The demand for EVs is currently at an exponential growth, meaning that the EVs are expected to be a significant part of the total market sales by 2030(i.e. 85 million EVs or 30% compared to 4.5% nowadays) [1]. Most of nowadays EVs to satisfy the requirements use Li-ion batteries because of several advantages: high specific energy, low self-discharge rate and long life-time [1] [2].

Based on different EV manufacturersâ descriptions, once EV batteries reach 70â80% of their nominal capacity, their role as EV first-life batteries is considered to be finalised. The reason behind this is that these kinds of batteries will result in lower mileage and safety concerns arise as the probability of a battery failure increases. Therefore, they do not meet the EV customer needs anymore. Usually, the batteries after their first life are discarded and recycled [1]. However, as the number of LIBs increases, recycling will not be able to cope with such a demand and thus environmental concerns arise [1] [3]. Thus, engineers and policymakers consider repurposing as a sustainable solution to this problem. Possible second life applications are ESS(Energy storage systems), grid stabilization, uninterruptible power supply(UPS), telecommunications towers and residential applications [4]. The decision of choosing between several applications relies on the State of Health (SOH) of these batteries at the time of re-purposing [4]. Moreover, SOH needs to be known as the modules with similar SOH need to be combined in new battery packs. This improves the 2nd life performance and reduces the battery pack failure rate [2].

The SOH conveys an approximate understanding of battery ageing and degradation behavior and also can be considered as an indicator of time, when the battery has to be reused or re-purposed. It essentially tells how a certain parameter or a combination of several parameters at the present state compare to the ideal state of the parameter/parameters of the LIB. Moreover, different applications may use different combinations of parameters to asses the SOH [5].

There are numerous challenges to determining the SOH of Li-ion batteries for their second-life. They can be classified as internal(related to the battery chemistry) and external(related to the environmental factors challenges). The Li-ion battery degradation mechanism is a complex process and has three modes, namely loss of lithium inventory, loss of active positive electrode material and loss of active negative electrode material, each of them having unique measurable effects on the battery health [4]. Also, due to different raw materials and products used in the manufacturing, the battery structures and physics differ, even though they have the same chemical composition. The external challenges are the operating conditions(temperature, humidity etc.) and they tend to cause different effects. Moreover, the unique driving patterns that create a dynamic load for the battery have unique impact on the batteries SOH as well [4].

Due to the exponentially increasing number of retired LIBs, rapid SOH estimation methods are more meaningful for the second life application. The rapid method involves evaluation of the health factors - the characteristic parameters that reflect the SOH. Examples of the health factor methods are electrochemical impedance spectroscopy(EIS), incremen-

tal capacity analysis(ICA or dQ/dV analysis), differential voltage analysis(DVA), differential thermal analysis(DTV), and sample entropy etc [6].

EIS method has numerous advantages compared to other SOH estimation methods. First of all, it is a rapid method and secondly, it gives the most detailed insight into the current battery state of health. The EIS reflects information about the internal resistance, solid electrolyte interface(SEI) layer, charge transfer resistance, double layer capacitance and diffusion processes. Each of these health factors indicates specific ageing processes. Thirdly, it is a non-destructive method and does not affect the operation of the battery [7]. On the other hand, EIS is an offline method and requires a steady state for the batteries meaning they have to be disconnected from any load or power source. Moreover, it requires advanced equipment as frequency response analysers(FRAs), potentiostats and/or voltage/current boosters.

A. *Research question*

Since most of the extracted modules from the EV have limited or no access to individual cells the EIS has to be performed on module level. However, most of the research is focused on performing EIS on individual cells. From the available literature two papers were found that used EIS on LIBs module level: [7] and [8]. However, there does not seem to be any study on the reliability of EIS on module level and how much information does each individual cell reflect on module measurement and this paper will have its focus on researching this. Additionally, EIS will be applied to get information about the SOH of aged Li-ion cells and module by comparison to the EIS of the same cells but in a new state.

The paper is structured as follows. The theory section includes background information about the EIS method and the current research of EIS on second-life Li-ion batteries and modules. In the method and experimental set-up section, a description of the technique used and the experimental set-up will follow. Next, the results are be presented, followed by an analysis and a discussion. Finally, conclusions are be drawn.

II. Theory&Literature review

A. *EIS theory*

Electrochemical impedance spectroscopy is a powerful and widespread electrochemical measurement technique. It essentially applies a small AC perturbation to the electrochemical cell and measures the response. The impedance can then be calculated, given that there will be a phase difference between the perturbation and the response. Different electrochemical processes are separated according to different time constants by sweeping the AC signal at different frequencies. Generally, the EIS can be performed in 2 different methods potentiostatic EIS(PEIS) and galvanostatic EIS(GEIS). In PEIS a small AC voltage is applied around the open circuit voltage(OCV) and the current response is monitored. In GEIS an AC current is applied and the voltage response is monitored [9]. For valid EIS measurements causality, linearity and time-invariance has to be maintained. To insure causality the response at time t has to be the result of the input before t and is not affected by other later signals. For maintaining linearity the AC signal has to be small, usually in the range of 5-20mV for Li-ion batteries [9]. In GEIS the current amplitude has to be chosen such that the resulting voltage signal is within this range. A depiction of the liner approximation for EIS is shown in Fig. 1.

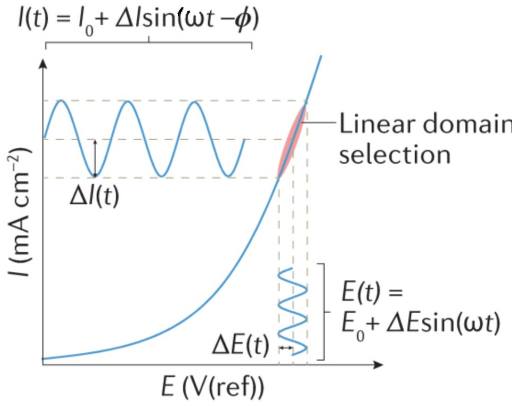

Fig. (1) *The linear region of EIS on the Butler-Volmer curve: if the applied AC voltage is kept small enough, the relation between the applied signal and the response is linear [10]*

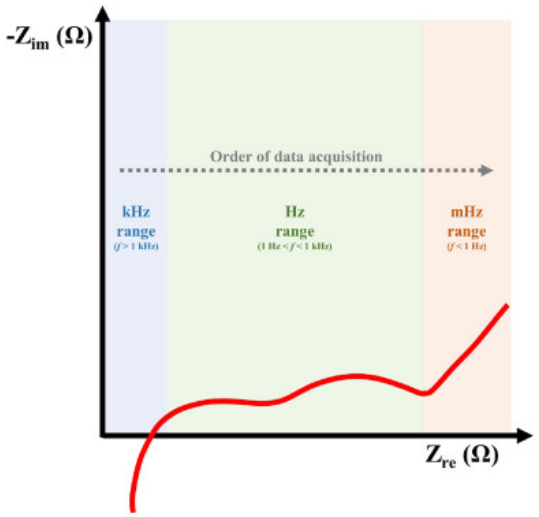

Fig. (2) *Graphical representation of a typical Li-ion cell EIS measurement displayed in a Nyquist plot [11]*

Time invariance can be maintained by allowing a relaxation time to the Li-ion batteries such that they reach a steady state. Any external disturbances are to be avoided. Thus, the output is only a result of the input.

PEIS is preferred for high impedance systems like coatings or corrosion-resistant materials. That is because low AC voltage signals applied to low impedance systems will result in high currents that usually exceed the current limitations of most of the potentiostats. Additionally, this may result in a poor SNR

ratio. On the other hand GEIS is used for low impedance systems with a current perturbation of usually in the 0.1â1 A range, resulting in a voltage response of a few mV that is well within the capability of most instruments [11].

The EIS calculates the impedance of the system for a range of frequencies, using the response to the perturbation. There are several ways to display the resulting impedance. The most common way is to plot it in a Nyquist diagram(where the imaginary part of the impedance is plotted against the real part) as shown in Fig. 2.

The Nyquist plot allows parametrization of the resistance, capacitance and inductance of the cell components and processes.

B. Equivalent circuit modelling(ECM)

A challenge for the EIS method is to analyze and interpret the results once the Nyquist spectra are obtained. The ECM way of interpretation of EIS results is the most used approach where different electrical circuit elements are assigned to the physical and chemical processes inside the cell. This method gives a broad insight about the Li-ion cell performance however its limitation is that it can lead to over-parametrization. Thus, it is important to only use elements that have an explainable physical or chemical process attributed to it. ECM is applied to the EIS spectrum by making a circuit model and adjusting its parameters to fit the simulated spectra to the measured one. It is an easy method to set-up with a low computational cost, thus suitable for battery management systems(BMSs). Moreover, it is used to analyse different states of Li-ion batteries by looking at changes of the parameters according to changes in SOC, SOH or temperature. The most common elements used in ECMs are resistors(R), inductors(I), capacitors(C), CPE(Q) and Warburg elements(W) [11].

A whole Li-ion battery can be modelled as shown in Fig. 3.

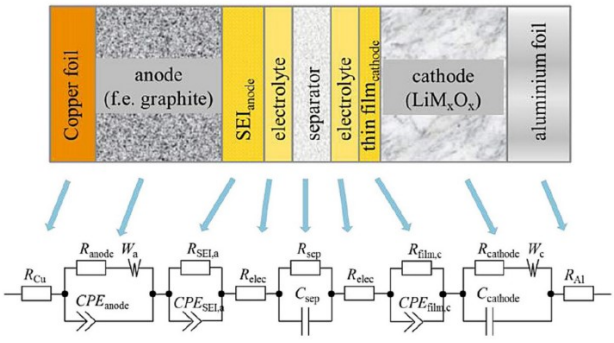

Fig. (3) *Entire circuit model of a lithium-ion battery [12]*

Due to the complexity of this model, for practical impedance analysis it needs simplification. To do this C_{SEP} is ignored as its value is minimal compared to the other capacitances. Moreover, the EIS spectra come mainly from the working electrode, so the elements attributed to the counter electrode can be safely ignored as well. Also, the series resistances R_{Cu}, R_{elec}, R_{Al} can be combined in one resistance. Thus, the overall simplified equivalent circuit of a lithium-ion battery half-cell is obtained [12]. The most common half-cell ECMs for Li-ion batteries is shown in Fig. 4.

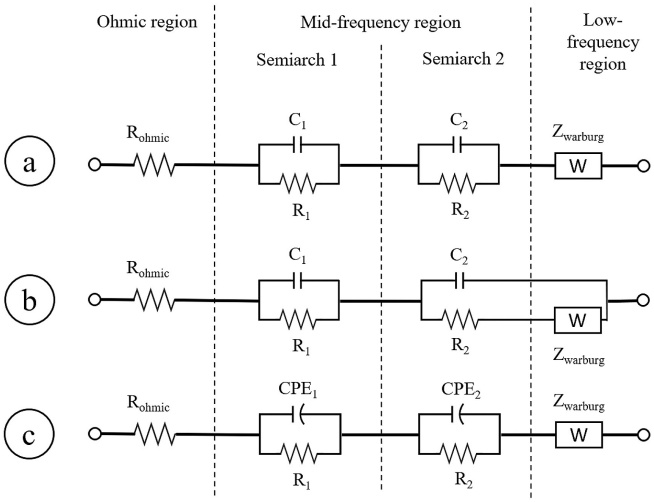

Fig. (4) *Common ECMs depending on Li-ion chemistry: a and b- mostly used for LCO cells, c- used for NMC and NCA cells [13]*

Regarding the EIS spectra, ECM differentiates 3 different regions in the complex plot(see also Fig. 2).

- high frequency range, $< 1kHz$- inductive effects(mostly due to the equipment, connecting wires and cell windings); usually modelled with an inductor and with a series resistance that represents the resistance of the electrolyte and electrode.
- Mid frequency range: parallel networks of resistors and capacitors(or CPEs) in series, that model charge transfer reactions, double layer effects at anodes, cathodes and solid electrolyte interfaces(SEIs). For LIBs 2 parallel networks of R and C(or CPE) are typically used.
- Low frequency range: diffusion processes modelled by Warburg elements or CPEs [11]

1) The role of CPE and Warburg elements: The constant phase element(CPE) was introduced in order to model the behaviour of a double layer which is an imperfect capacitor. In a Nyquist plot an ideal parallel RC element would show as a semicircle with the radius on the x-axis. However, in real life electrochemical systems it was noticed that the center sometimes is bellow the x-axis, that is a result of the double layer effect [14]. The electrical impedance of the CPE is:

$$Z_{CPE} = \frac{1}{Q_0(j\omega)^n} \tag{1}$$

, with $0 < n < 1$. Q_0, has no physical meaning, however in the case of parallel CPE and a resistor(R) the actual capacitance can be calculated as:

$$C = \frac{(RC)^{1/n}}{R} \tag{2}$$

, as long as $n > 0.75$. Warburg element is used to model diffusion processes in electrochemical systems. It is essentially a CPE with $n = \frac{1}{2}$. Its impedance is given by:

$$Z_W = \sigma \frac{1}{\omega^{1/2}} - j\sigma \frac{1}{\omega^{1/2}} \quad (3)$$

2) The link of ECM elements to degradation processes inside LIBs: The degradation processes of LIBs have particular effects on each of three regions in the EIS spectrum. The most common ones are:

- Resistive region: modelled by a resistor. The degradation process linked to it is the electrolyte decomposition cause by loss of lithium inventory.
- Mid-frequency region: two semiarches can be distinguished, each one modelled by a parallel CPE and resistor. The first one is linked to loss of anode active material, loss of lithium ions that lead to solid electrolyte interface(SEI) layer growth and decomposition. Typically, the elements are noted as R_{SEI} and CPE_{SEI}. The second one is linked to loss of cathode active material and charge transfer slowdown. Typically, the elements are noted as R_{ct} and CPE_{dl}(to denote the charge transfer(ct) process and double layer(dl) effects).
- Low-frequency region: modelled by Warburg or CPE element and they are linked to loss of cathode active material and to changes in electrodes structure [13].

The degrdation processes linked to the ECM elements are shown in Fig. 5.

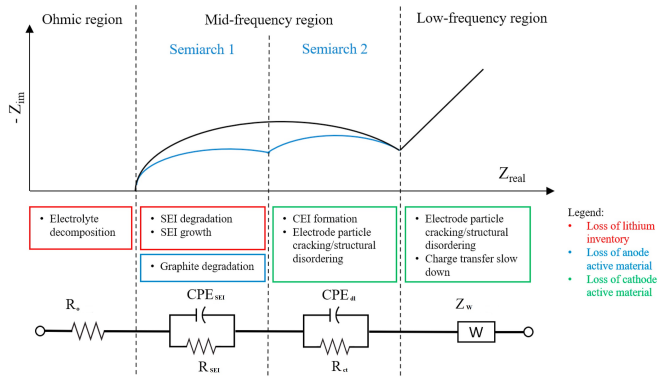

Fig. (5) *LIBs degrdation processes linked to the ECMs elements [13]*

C. Present research on EIS on LIBs

Most of the research is focused on applying the EIS on LIBs on cell level and analysing how the ECMs elements change after changes in the SOC, SOH and temperature. Paper [7] quantified the degree of correlation between ECM elements to SOC, SOH and temperature. It found that R_o and R_{ct} are strongly correlated to SOH with a correlation quotient(pearson's r correlation matrix) of 0.949 and 0.849 respectively. The CPEs Q_0 showed less correlation to the SOH due to the fact that the CPE is linked to capacitive effects that have less correlation to SOH than the resistive ones. The Q_0 showed the highest correlation to the SOC and temperature of the battery instead. This research was done on cell level.

Paper [6] used EIS on module level, only up to 3 cells in series and superimposing the results to get the full module sepctra. It found that the sum of the ohmic resistance and SEI resistance($R_0 + R_{SEI}$) can be a health factor for off-line SOH esstimation of LIB modules.

Other papers found similar results. For instance, paper [11] found the same trend of increasing resistance with ageing. From Fig. 6 it can be clearly seen that R_o and R_{ct} both increase with ageing(an increase in R_{ct} being attributed to an increase in the semiarc).

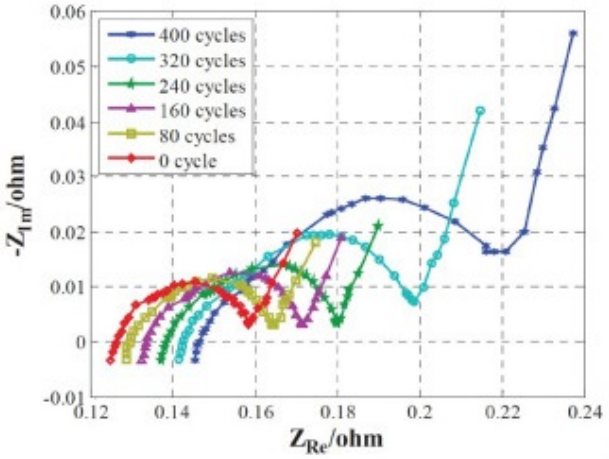

Fig. (6) *Lithium cobalt oxide batterys effect of ageing on the EIS spectra [11]*

III. Method and Experiment set-up

A. Method description

EIS is be performed on 6 new cells(100% SOH) separately, and then for series module of 2 till 6 cells. The measurements are performed at 100% SOC. The same measurements are performed for 6 aged cells at about 93%SOH. Subsequently, an electrical model is chosen according to the battery chemistry and fitting simulations are performed. The ECM elements are then parametrized and the results are recorded. For each added cell the expected ECM elements values for the module are calculated and compared to the measured one. Furthermore, it is analysed at what extent each cell reflects at module level.

The ECM element values are compared at different SOH, by comparing the new and the aged cells and modules. The parameters that show the highest sensitivity to SOH change are analyzed.

B. Measurements equipment

For performing the EIS measurements Solartron Echem-Lab XM is used, which is equiped with a potentiostat / galvanostat, frequency response analyzer(FRA) and optional high voltage(HV) amplifier. The potentiostat has a voltage span of $\pm 8V$ and a current span of $\pm 300mA$. The frequency range of the FRA is $10\mu Hz - 1MHz$. The High Voltage

option has a voltage span of $\pm 100V$ with a current span of $\pm 100mA$. Since the voltage of the Li-ion module ranges from 19.2V-25.2V, the HV option of the solartron is used [15]. It has 4 main and 4 auxiliary channels. Since the EIS is performed in galvanostatic mode, the following channels are used with the described purpose:

- WE-is connected to the working electrode(cathode) of the cell and monitors the current
- CE-is connected to the counter electrode of the cell and provides a current(or voltage) to drive the cell
- RE-connects a pair of reference electrode points(RE1 and RE2) across the cell to monitor the voltage difference between those points

So, in galvanostatic mode CE applies an AC current, WE monitors the applied current and RE monitors the AC voltage response [15]. The schematic level set-up is shown in Fig. 7

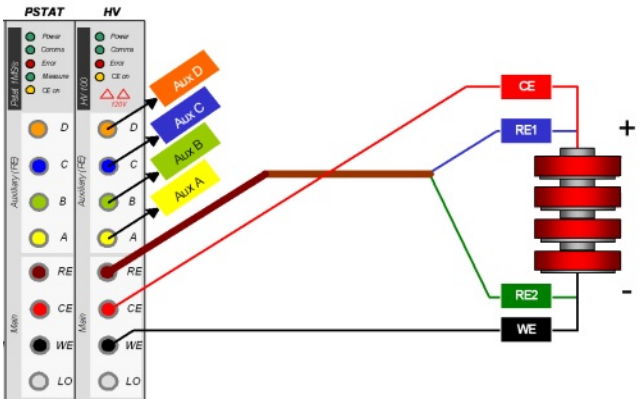

Fig. (7) *Schematic of the set-up and connections between Solartron and the battery module; in the actual set-up 6 cells in series are used [15]*

C. Battery module and cell set-up

For the measurements 6 aged and 6 new Panasonic NCR18650PF Li-ion batteries will be used. The number of cycles and the use conditions of the aged batteries is unknown. The new battery capacity is 2750mAh with an operating voltage between 3.2V to 4.2V. Thus, a battery with 3.2V will be considered at 0%SOC and 4.2V at 100%SOC. In this paper the temperature of the batteries will be considered room temperature, $20°C$ and is left constant. The 6 old batteries were welded in series into a module and the same was done for the 6 new cells. The battery/module connections with the equipment are very important in order to have reproducible results. First of all, the welding of the batteries helps by making sure that the contact resistance between batteries does not vary. Secondly, the same connectors have to be used for each measurement. In this experiment banana plugs cables from solartron were connected to banana sockets welded on each battery cell. The experimental set-up is shown in Fig. 8.

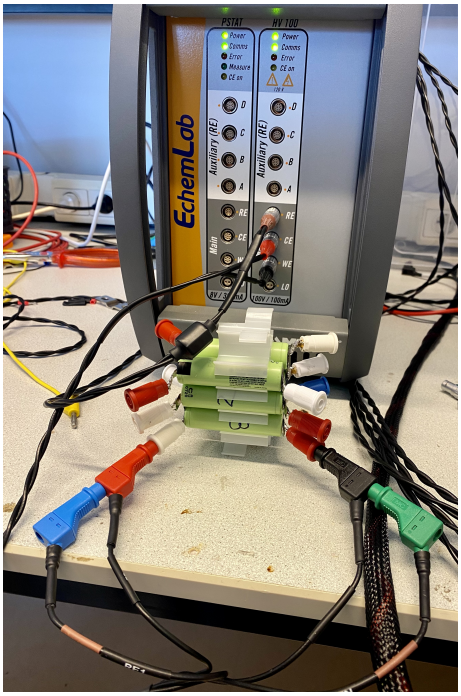

Fig. (8) *The set-up to perform EIS measurement by Solratron EchemLab potentiostat/galvanostat instrument on module with 6 Li-ion cells*

D. EIS experimental parameters

The Li-ion batteries have a low impedance and for low impedance systems GEIS is preferred because present potentiostats have more current ranges than voltage ranges and doing the EIS for low impedance in the current mode gives more accurate results [16]. Also, for the batteries used in these measurements the exact impedance is not known at the beggining, meaning that GEIS has to be used to prevent getting large amplitude currents that can potentially over-excite the battery or go over the equipment current limit(that can usually happen for PEIS for low impedance systems).

1) GEIS frequency range and AC current amplitude choice: The frequency range that is chosen for these batteries is 10kHz-20mHz. This was proved to cover the 3 EIS regions making it possible to perform the ECM. To chose an appropriate current amplitude for GEIS the following steps are undertaken:

1) First, a GEIS test with half of the maximum equipment current is performed on one new cell and the whole new 6 cell module. This reflects the battery impedance and then adjustments on the current amplitude can be made. Thus, the used current for this test was 35mA RMS, or 50 mA amplitude.
2) The ohmic impedance of one new cell is determined: $23m\Omega$. The resulting voltage amplitude is therefore $23m\Omega \cdot 50mA = 1.15mV$. Given that the lowest range for the Solartron HV option is 37mV the current amplitude has to be increased. The maximum current amplitude of 100mA will then be chosen to achieve the maximum accuracy with the HV option.

3) To check if 100mA current amplitude operates the module and the cells in the linear mode an FFT and harmonic analysis has been done.

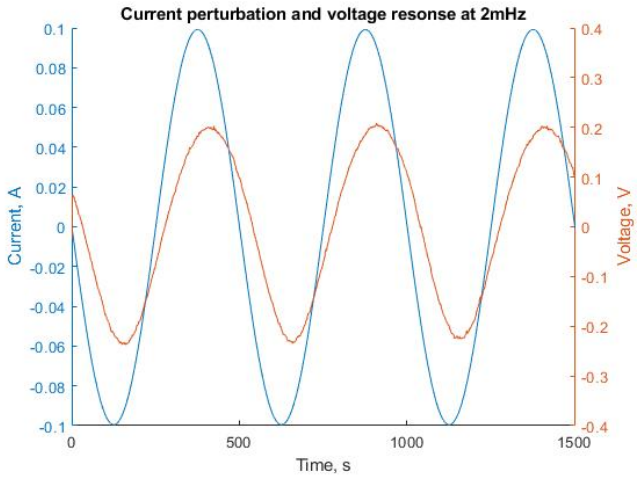

Fig. (9) *100 mA AC current perturbation and voltage response at 2mHz on 6 Li-ion cells module connected in series*

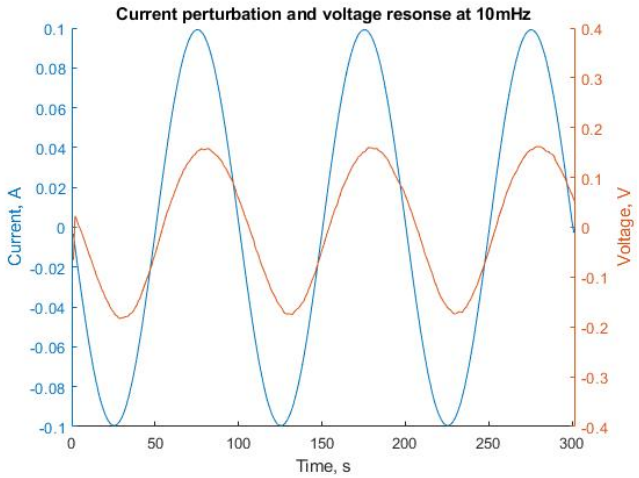

Fig. (10) *100 mA AC current perturbation and voltage response at 10mHz on 6 Li-ion cells module connected in series*

For the linearity check a single sine test for the worst case scenario is done. The single sine test applies a single frequency AC current and the monitors the AC voltage response. The worst case scenario is the lowest frequency tested, since at that frequency the impedance is the highest, resulting in the highest AC voltage amplitude on the whole frequency range. If the THD at that frequency is low the EIS can then be considered linear for the whole frequency range. The FFT on the AC voltage response of 6 new cells in series is performed and the THD is calculated at 2mHz and 10mHz. The plots are shown in Fig. 9, 10 and Fig. 11, 12.

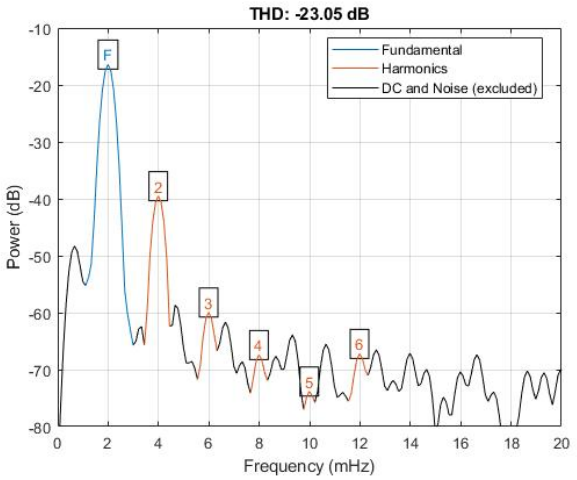

Fig. (11) *FFT and THD of resulting AC voltage after 100 mA AC current perturbation at 2mHz on 6 Li-ion cells module connected in series*

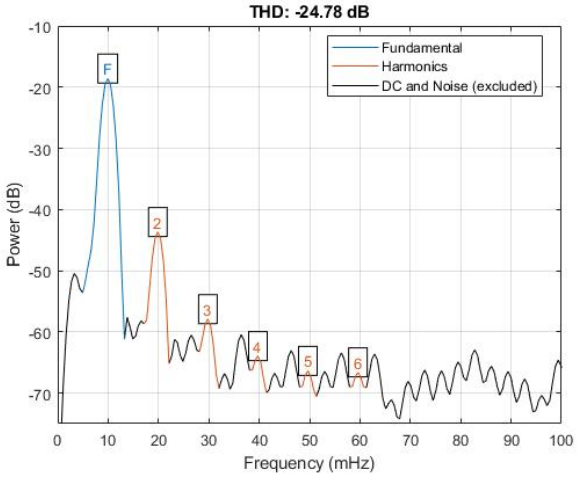

Fig. (12) *FFT and THD of resulting AC voltage after 100 mA AC current perturbation at 10mHz on 6 Li-ion cells module connected in series*

At 2mHz and 10mHz the THD in percentage is 6.5% and 5.7% respectively, Fig. 11, 12. These THD levels validate the AC current choice and that the EIS will be linear for the whole frequency range.

E. EIS Li-ion model implemented

The EIS fitting analysis is performed with ZView software. Two models are experimented with. The usual model for the NMC Lithium-ion in Fig. 13 shows better curve fit, however the error for the resistive parameters is too high($> 10\%$). A better accuracy for the resistors is obtained with the model in Fig. 14. This model is applied in the end for analysing the EIS spectra.

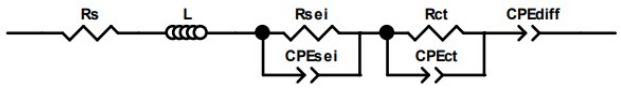

Fig. (13) *The Li-ion equivalent circuit model typically used for NMC battery chemistry*

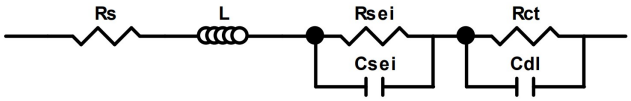

Fig. (14) *The Li-ion equivalent circuit model used for curve fitting technique in this paper*

IV. Results&Discussion

A capacity test is performed for the aged cells to get a starting reference and a first insight into the SOH of the cells. The capacity compared to 100% SOH is shown in Fig. 15. The cells are at a good SOH ranging from 95%-99%.

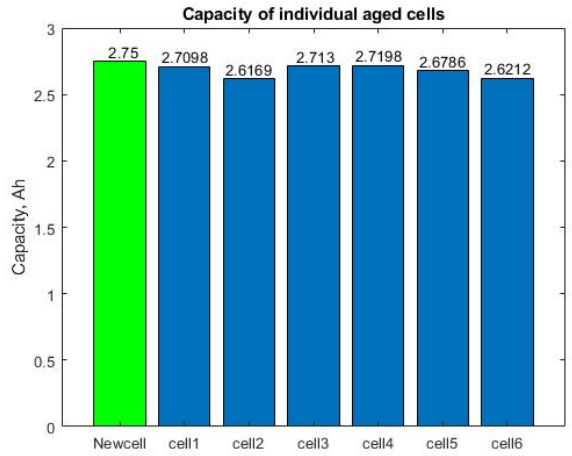

Fig. (15) *Capacity of aged cells compared to a new cell*

The EIS spectra for individual new and aged cells in Fig. 16 and 17 can be compared. Both spectra show the 3 distinguishable regions typical for Li-ion battery: the inductive region, capacitive region(2 semi-arcs) and the diffusion region. The spectra for the aged cells are shifted to the right showing an increase in the ohmic resistance. The main cause of this is the decomposition of the electrolyte over time that leads to an increase in the internal resistance of the battery [7]. Furthermore, the radii of the aged cell 2,3,4,5,6 spectra is increased. This relates to an increase in the charge transfer resistance, R_{ct}. The main cause for this lies in the fact that R_{ct} is linked to the lithium diffusion to the electrodes. As the cell ages, the SEI layer thickens, thus increasing the barrier for the lithium and decreasing the diffusion rate [7].

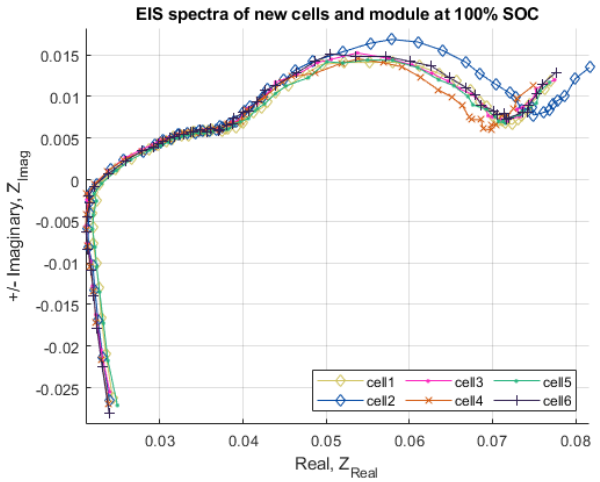

Fig. (16) *EIS spectra of new individual cells at 100% SOC*

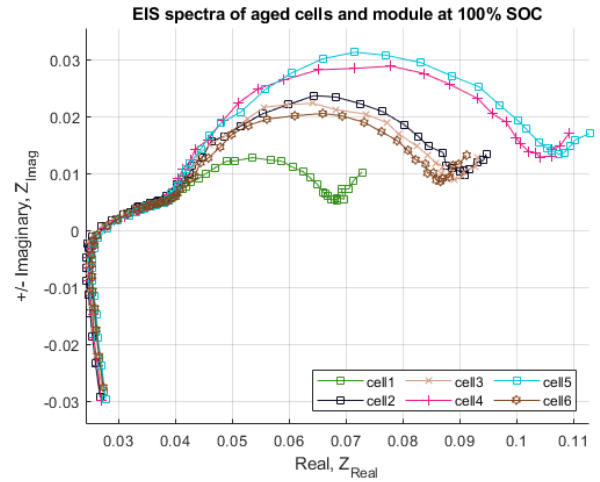

Fig. (17) *EIS spectra of aged individual cells at 100% SOC*

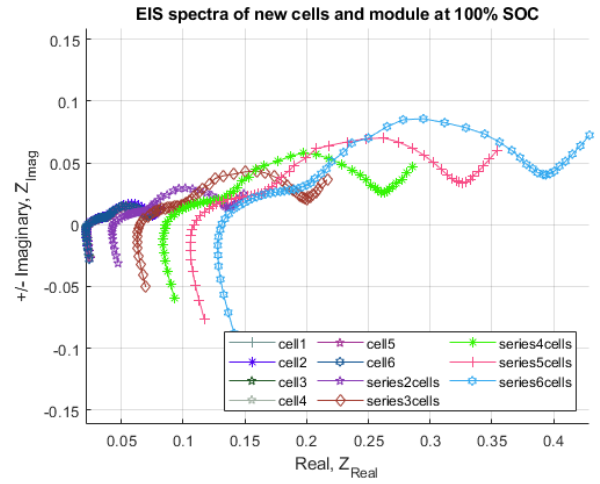

Fig. (18) *EIS spectra of new single and series cells at 100% SOC*

TABLE (I) *New li-ion module and individual cells parameters at 100% SOC*

Parameters / Tested	$R_s, [m\Omega]$	$R_{SEI}, [m\Omega]$	C_{SEI}, mF	$R_{ct}, [m\Omega]$	C_{dl}, F
$1^{st} cell$	23,1	15,6	47,3	33,6	3,82
$2^{nd} cell$	22,49	15,5	45,53	37,7	3,87
$3^{rd} cell$	22,09	15,29	42,97	34,5	3,83
$4^{th} cell$	22,2	14,9	43	32,5	3,57
$5^{th} cell$	23,1	15,38	42,7	33,7	3,77
$6^{th} cell$	22,3	15,2	45,1	35,09	3,95
2 series cells(1,2)	44,8	25,28	38,1	67,9	1,96
3 series cells(1,2,3)	65,8	35,1	29,8	99,7	1,28
4 series cells(1,2,3,4)	87,69	45	24,5	131	0,95
5 series cells(1,2,3,4,5)	110,3	55,3	19,9	161,9	0,75
6 series cells	133,5	65,7	17,7	197,2	0,63
Individual cells combined	135,28	91,87	7,3	207,09	0,64

TABLE (II) *Aged li-ion module and individual cells parameters at 100% SOC*

Parameters / Tested	$R_s, [m\Omega]$	$R_{SEI}, [m\Omega]$	C_{SEI}, mF	$R_{ct}, [m\Omega]$	C_{dl}, F
$1^{st} cell$	25,6	13,4	37,7	29,2	3,4
$2^{nd} cell$	25,3	13,6	46,3	50,9	4,04
$3^{rd} cell$	25,34	13,3	42,8	49,7	3,76
$4^{th} cell$	25,45	13,2	38,8	64,7	3,72
$5^{th} cell$	26,2	13,3	44,2	66,9	3,93
$6^{th} cell$	26	13,5	38,39	46,6	3,7
2 series cells(1,2)	51,48	22,1	38,5	77,6	2,01
3 series cells(1,2,3)	75,7	30,4	30,64	126,3	1,32
4 series cells(1,2,3,4)	101,1	38,8	26,9	189,3	0,99
5 series cells(1,2,3,4,5)	126,5	47,18	23,78	254,5	0,8
6 series cells	152,5	55,7	20,5	302,8	0,65
Individual cells combined	153,89	80,3	6,85	308	0,63

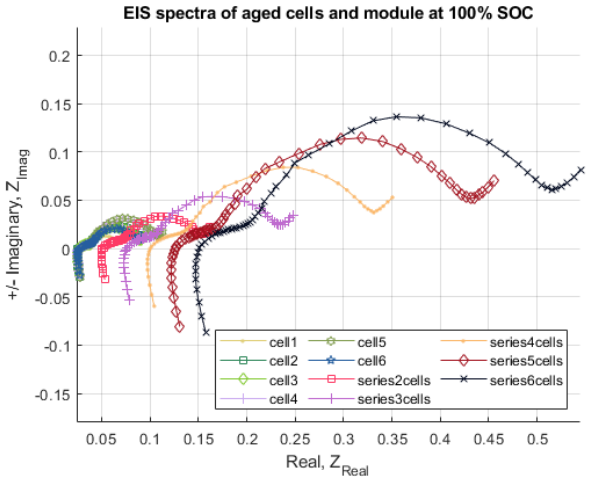

Fig. (19) *EIS spectra of aged single and series cells at 100% SOC*

To assess the contribution of each cell to the whole 6 series cells module the EIS was measured for each added cell in series. The spectra for the new and old cells are depicted in Fig. 18 and Fig. 19. The spectra are equally spaced on the real axis. Since the individual cells have about the same internal resistance this means that on the module level the internal resistance can be accurately assessed from the EIS. To quantitatively assess this for the internal resistance and other ECM parameters, curve fitting technique will be performed in ZView software.

The parameters used from the model in Fig.14 are: internal resistance(R_s), SEI resistance(R_{SEI}), SEI capacitance(C_{SEI}), charge transfer resistance(R_{ct}), double layer capacitance(C_{dl}). The inductive part was left aside as it is strongly influenced by the equipment internals and cell interconnections and it does not give meaningful information about the battery state. The R_{SEI} and C_{SEI} can be linked

to the first semiarc. Subsequently, R_{ct} and C_{dl} can be linked to the second semiarc. This is because R_{ct} is the largest among the total resistance for the lithium-ion battery and as seen in Table I and Table II the resistance linked to the second semi arc is the largest among the others [13]. Furthermore, for the new module the internal resistance has a 1% deviation compared to the sum of each single cell's resistance. Similarly, the charge transfer resistance and double layer capacitance of the whole module has a 4.77% and 1.5% deviation compared to the combined R_{ct} and C_{dl} of each single cell. Similar deviations were obtained for the aged module. The small deviations can be caused by the equipment and fitting algorithms errors.

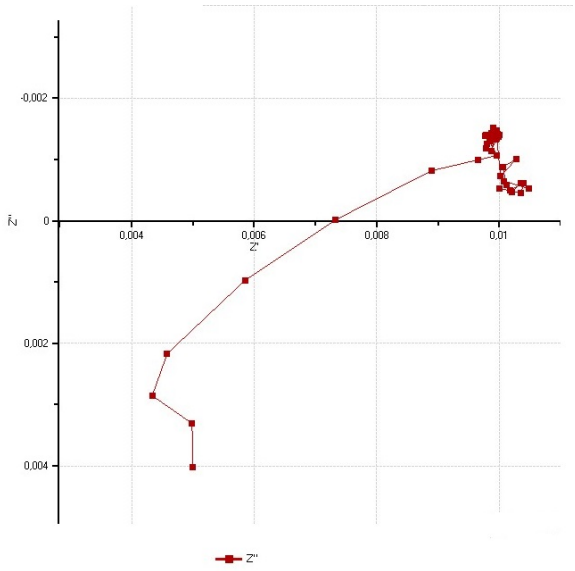

Fig. (20) *The measured HV noise on a low impedance cell out of the equipments measuring range*

However, this was not the case for the R_{SEI} and C_{SEI}. The R_{SEI} and C_{SEI} of the whole module is clearly not the combined R_{SEI} and C_{SEI} of each single cell. The cause for this can be due to an influence from the counter electrodes that is ignored in the half cell ECM system. However, no explanation of this was not found in the literature. Another cause for this deviations could have been the noise of the HV option at higher frequencies. A trial to explain this was done by substracting the 6 cells EIS spectrum from the combined EIS spectra of the individual cells. The resulting plot would be the noise of the equipment. To compare this to the actual noise of the HV option an EIS test was done on a very low impedance cell that is not within the range of the HV measuring equipment. The plots in Fig. 21 and 20 showed to be similar meaning that the HV noise could have been indeed the cause of the deviations for R_{SEI} and C_{SEI}.

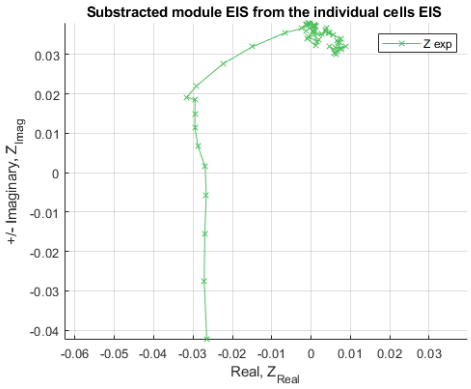

Fig. (21) *The 6 cells module EIS spectrum substracted from the combined EIS spectra of the individual cells*

From table I and table II the parameters that showed the highest sensitivity to the change in SOH are R_{ct} and R_s. The double layer capacitance does not show significant changes to an SOH alteration. Same parameters were shown to have the highest correlation to SOH in [7]. They were plotted in Fig. 22 and Fig. 23. The R_{ct} shows a higher sensitivity, meaning it could be possibly used to detect small changes in SOH of lithium-ion batteries/modules.

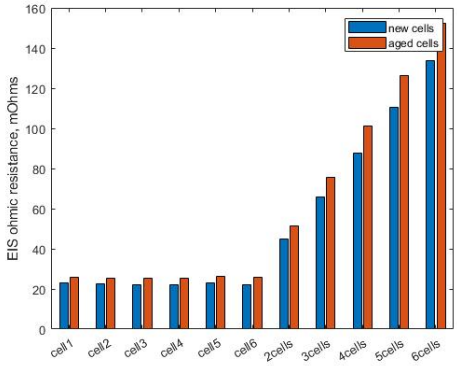

Fig. (22) *Ohmic resistance of aged and new cells and modules*

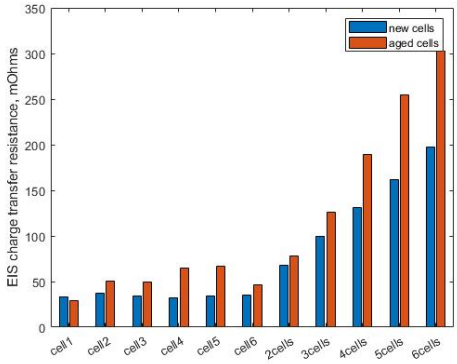

Fig. (23) *Charge transfer resistance of aged and new cells and modules*

V. Conclusion

In this paper EIS was performed on a new and an aged lithium-ion 6 cells module to assess the contribution of single cells to the whole module's EIS. The EIS was performed in galvanostatic mode with a 100mA AC current due to the low impedance of the lithium-ion cells. A linearity check was done by performing a FFT on the resulting AC voltage after a 100mA AC current perturbation on the 6 cells module. The THD calculated was 5%, thus validating the current amplitude choice. Furthermore, to improve the contact resistance and the reproducibility of the EIS measurements welding was used to connect the cells. Fitting of impedance spectra via an ECM for single cells and at each point in the module allowed the components to be analyzed. The internal resistance, charge transfer resistance and double layer capacitance of single cells accurately reflected on the module EIS measurement, with errors of 1%, 4.77% and 1.5% respectively. The SEI resistance of the module was less than expected considering each cells SEI resistance. Similarly, the SEI capacitance of the module showed a different value than the combined SEI capacitance of each cell. A trial to explain this was done and it was shown that the reason could be the noise of the equipment's HV option at higher frequencies. Additionally, the aged module's SOH was assessed by determining the sensitive components and making comparisons with the new module. The internal resistance of the aged cells and module showed an increase of 12%. The charge transfer resistance showed to be more sensitive to the SOH alteration with an increase of 32.8% for the module meaning it could possibly be used to detect small changes in the batteries and modules SOH.

The results show that the EIS can be accurately performed on lithium-ion modules and analyzed using the ECM internal resistance, charge transfer resistance and double layer capacitance.

A. Future work

Future work could be continued on the EIS on module level. It can be studied how does the AC current amplitude influence the accuracy of the EIS on module level. Also the research could focus on algorithms to determine single bad cells from the EIS on lithium-ion modules. Furthermore, correlation analysis between the EIS and the battery states(SOC, SOH and temperature) can be performed on module level.

Acknowledgment

I thank my supervisors ir. Reza Azizighalehsari and dr.ir. Prasanth Venugopal for their assistance and support during the time of the thesis. I also thank the lab technician ir. Roelof Grootjans for technical support with all the equipment used.

References

[1] M. Hussein, J. W. Lee, G. Ramasamy, E. E. Ngu, S. P. Thiagarajah, and Y. H. Lee, "Feasibility of utilising second life EV batteries:Applications, lifespan,economics, environmental impact, assessment, and challenges," *Alexandria Engineering Journal*, vol. 60, p. 4517â4536, 2021.

[2] N. Horesh, C. Quinn, H. Wang, R. Zane, M. Ferry, S. Tong, and J. C. Quinn, "Driving to the future of energy storage: Techno-economic analysis of a novel method to recondition second life electric vehicle batteries," *Applied Energy*, vol. 295, 2021.

[3] X. Wang, G. Gaustad, C. W. Babbitt, C. Bailey, M. J. Ganter, and B. J. Landi, "Economic and environmental characterization of an evolving Li-ion battery waste stream," *Journal of Environmental Management*, vol. 135, pp. 126–134, 2014.

[4] A. Basia, Z. Simeu-Abazi, E. Gascard, and P. Zwolinski, "Review on State of Health estimation methodologies for lithium-ion batteries in the context of circular economy," *CIRP Journal of Manufacturing Science and Technology*, vol. 32, p. 517â528, 2021.

[5] M. Shahjalal, P. K. Roy, T. Shams, A. Fly, J. I. Chowdhury, M. R. Ahmed, and K. Liu, "A review on second-life of Li-ion batteries: prospects, challenges, and issues," *Energy*, vol. 241, 2022.

[6] Q. Zhang, X. L. Z. Du, and Q. Liao, "Aging performance characterization and state-of-health assessment of retired lithium-ion battery modules," *Journal of Energy Storage*, vol. 40, 2021.

[7] K. M. Carthy, H. Gullapalli, K. M. Ryan, and T. Kennedy, "Electrochemical impedance correlation analysis for the estimation of Li-ion battery state of charge, state of health and internal temperature," *Journal of Energy Storage*, vol. 50, 2022.

[8] F. L. Daniel Kehl, Torben Jennert and M. Kurrat, "Electrical characterization of li-ion battery modules for second-life applications," *MDPI*, vol. 32, 2021.

[9] H. Watanabea, S. Yoshina, H. I. Shitanda, and M. Itagaki, "Electrochemical impedance analysis on positive electrode in lithium-ion battery with galvanostatic control," *Journal of Power Sources*, vol. 507, 2021.

[10] O. G. V. V. M. G. . M. E. O. Shangshang Wang, Jianbo Zhang, "Electrochemical impedance spectroscopy," *Nature Reviews Methods Primers*, vol. 41, 2021.

[11] F. O. J.-S. L. V. R. E. N. S. S. G. H. R. R. M. G. J. P. Nina Meddings, Marco Heinrich, "Application of electrochemical impedance spectroscopy to commercial Li-ion cells: A review," *Journal of Power Sources*, vol. 480, 2020.

[12] W. Choi, H.-C. Shin, J. M. Kim, J.-Y. Choi, and W.-S. Yoon, "Modeling and applications of electrochemical impedance spectroscopy (eis) for lithium-ion batteries," *Department of Energy Science*, vol. 440, 2019.

[13] P. Iurilli, C. Brivio, and V. Wood, "On the use of electrochemical impedance spectroscopy to characterize and model the aging phenomena of lithium-ion batteries: a critical review," *Journal of Power Sources*, vol. 505, 2021.

[14] M. Lacey. The constant phase element. [Online]. Available: http://lacey.se/science/eis/constant-phase-element/

[15] A. Solartron analytical, "User guide," 2016.

[16] Gamry. Eis measurement of a very low impedance lithium ion battery. [Online]. Available: https://www.gamry.com/application-notes/EIS/eis-measurement-of-a-very-low-impedance-lithium-ion-battery/